Parametric analysis of the structural response of steel base plate connections

M.J. Kontoleon, E.S. Mistakidis, C.C. Baniotopoulos*, P.D. Panagiotopoulos [1]

Institute of Steel Structures, Department of Civil Engineering, Aristotle University, 54006, Thessaloniki, Greece

Abstract

The present paper aims to contribute to the parametric analysis of semirigid steel base plate connections. The method is based on the theoretical results of nonsmooth mechanics, which is a relatively new branch of mechanics initiated three decades ago and deals with problems from mechanics and/or structural analysis that involve generalizations of the gradient. The numerical modelling of the structural response of a steel column base plate under static loading where unilateral contact with friction and yielding phenomena are taken into account, could be considered as a typical problem that can be very effectively treated within such a theoretical framework. In particular, the respective stress states of the steel connection under static loading are calculated by taking into account the development of plastification zones and the unilateral contact and friction effects on the interfaces between connection members. An effective two-dimensional finite element model, capable of describing the previously mentioned phenomena is constructed. The aforementioned model is a simplification of the respective three-dimensional one and aims to reduce in a reliable way the huge computational effort required for the analysis of three-dimensional fine meshes of discretized steel connections. A numerical application demonstrates the effectiveness and the applicability of the method altering two parameters, the base plate thickness and the axial load of the model. © 1999 Elsevier Science Ltd. All rights reserved.

1. Introduction

Classic methods for the calculation of steel connections have assumed complete contact between the interfaces. For the last few years, this assumption has been widely used for the study of steel column base plate connections because it generally leads to conservative results. In the case that a load leading to the development of moment, shear and tension is applied, this assumption fails to describe the actual response of

the base–steel plate interface. Laboratory tests and construction practice prove that separation is often caused on the contact surface, between the deformable column base plate and the rigid concrete foundation. This phenomenon has already in recent years attracted the interest of numerous researchers who have applied analytical, experimental and numerical approaches to investigate it. The analytical approaches which have been considered, on the column base plate effective contact surface, where various normal reaction distributions appear in the presence of concentric and/ or light loading [1–3] are significant. Extensive experimental investigations, aiming at accurate description and evaluation of the response of column–base connections, have been conducted for concentric and

---

* Corresponding author
[1] Also at the Faculty of Mathematics and Physics, RWTH, 52062 Aachen, Germany.

eccentric loads [4–7]. Finally, the numerical approaches based on the finite element method and the boundary element method have been applied for the analysis of column base plate connections [8]. In recent years, numerical simulations of steel connections have been described by one- to three-dimensional models. The one-dimensional (Bernoulli beam) models of such connections (bolts modelled as springs), taking into account only primary bending action, are naturally the most simple. On the other hand, a three-dimensional model can incorporate all the essential features of the steel connections, leading in general to the most accurate results. This is due to the fact that three-dimensional models, having been appropriately formulated and computed, contain the correct stress distribution patterns, but in a form that requires great computational effort.

Between the two above-mentioned models, two-dimensional models have been proposed, offering the following advantages: (i) accurate numerical results in the cases where the geometry connections and the loading conditions lead to two-dimensional deformed configuration; (ii) minimum computational cost and evaluation save effort; (iii) applications for quick benchmark tests in validating commercial three-dimensional finite element codes, for the analysis of steel connections.

The first attempts for two- and three-dimensional modelling of steel connections, based on several simplified assumptions, date back to the seventies; these efforts have been continued to date by deducting one by one the simplifying hypotheses of the initially proposed models, thus producing more and more interesting and realistic results [9–17].

In the present paper, a two-dimensional finite element plane stress model is constructed for the parametric analysis of the structural behaviour of a column–base plate connection. The model contains all the essential features that characterize the separation problem. Material yielding, contact interface slip and interface interaction are taken into account. Secondary bending effects are not present due to the static loading. The third dimension of the connection is also considered by assigning different thickness values to the various regions of the FEM mesh.

The numerical method proposed herein does not use any a priori assumption on the flexibility of the several parts of the steel connection to obtain first its deformed shape where contact (i.e. compressive reaction) and separation (i.e. tensile reaction) zones have been developed, and then the actual stress distribution on the connection members by taking into account friction effects on the interfaces (cf the PANA-method, for example [18,19]). By means of this numerical method, friction forces are also taken into account on all the interfaces of the steel connection applying a double-step iterative numerical procedure. In particular, solving iteratively first a unilateral contact problem for the steel connection in the presence of friction forces and next a friction problem in the presence of normal reaction forces computed in the previous solution step, the deformed shape of the connection (that includes all the contact, non-contact and plastified zones) and the actual stress distribution are accurately defined. Then, using the existing standards and norms, the design of the connection at hand can be easily completed. The proposed finite element model is constructed in a way that the interaction at any interface of the connection can be taken into account by means of unilateral contact boundary conditions [20–23].

Following this method, local separation zones between the interfaces of the steel connection are computed, whereas the deformed shape of the steel connection is evaluated with accuracy. Introducing the unilateral contact law with friction to simulate the boundary conditions on the steel connection interface, the separation process can be mathematically described giving rise either to a primal quadratic programming problem with respect to the displacements, or equivalently to its dual formulation with respect to the stresses. As has been proved [18,23] the primary problem expresses from the standpoint of mechanics, the principle of the minimum of the potential energy of the connection under consideration at the state of equilibrium, whereas the dual one uses the principle of the minimum complementary energy. Solving iteratively these two problems and using the output of the former as input for the latter, the method converges after a few steps to the actual solution of the problem (as proved by means of a fixed point algorithm [24]). The transformation of the initial structural steel connection problem into a sequence of constrained quadratic programming problems makes things from a computational point of view much simpler and allows for the application of a wealth of theoretical work and software. Note that the numerical results calculated by applying the proposed two-dimensional model qualitatively conform well to those obtained by experiments [25,26]. Within such a theoretical framework, the separation and the active contact, as well as the plastification zones are calculated with accuracy, leading thus to the computation of the exact stress state conditions holding on the steel connection under investigation.

The proposed numerical method, seems to be a reliable tool for the numerical simulation of the structural behaviour of most types of steel connections, because for one side the response of the different parts (column, plate, bolts) of the modelled steel connections are taken into account in an interactive way, whereas on the other side, the correct thicknesses of the various parts of the two-dimensional model are defined by applying an efficient and easy technique [27].

The numerical treatment of such problems, presented in a form of quadratic programming, also permits the investigation of the appearance of prying action. In the case of the column–base plate connection, the prying action phenomenon is directly connected to the flexibility of the connections. In flexible connections, e.g. in splice plates, such forces do not appear. The reaction is the exact opposite in the case of steel column–base plates with underlying concrete foundation. The difference is due to the fact that one part of the connection (concrete foundation) is not deformable and this causes the deformable base plate to be locally separated from the concrete surface. As is obvious, the thickness of the base plate, is one of the most significant parameters that affects the response of such steel connections. Therefore, considering the thickness as a critical parameter for the analysis of the connection interface, under various axial external forces and moment rotation, such a parametric analysis should be considered as a contribution to the research of steel column–base plate connections. The parametric study of a numerical application is presented in the last part of the paper, taking into account the base plate thickness as a parameter for analysis of the connections described above. The obtained results are of great interest, showing the different response of each connection of different base plate thickness under different loading conditions.

2. Mathematical description of the method

A steel connection composed by several structural elements such as plates, bolts, etc. is first considered (Fig. 1). Moreover, we assume that the material of the parts of the connection (which may be different for the various parts, e.g. high strength steel for the bolts, mild steel for the plates, etc.) exhibits an elastoplastic behaviour, with or without hardening. Between the various parts of the connection, certain interfaces are formed which in the following are denoted by Γ_S. The forces applied on the connection are transmitted by the interfacial forces developed on the parts of the connection which come into contact. These forces are the contact forces which develop normal to the interface direction, and the frictional forces which develop tangential to the interface direction, and only between those parts that come into contact.

The unilateral contact conditions on the interfaces are mathematically expressed by the following form:

if $[u_N] > 0$ then $S_N = 0$ and if $[u_N] = 0$ then

$$S_N \geq 0 \tag{1}$$

where S_N denotes the contact pressure and $[u_N]$ are the

relative displacements normal to the interface. This relation holds for every one of the k nodes of the discretized structure which belongs to the interfaces Γ_S. Furthermore, the friction boundary conditions holding on the active contact regions (defined by the right-hand part of Eq. (1)) are expressed in the following form:

if $[u_T] = 0$ then $|S_T| < \mu |S_N|$ and

if $|[u_T]| > 0$ then $|S_T| = \mu |S_N|$ \tag{2}

where μ is the Coulomb's friction coefficient and $[u_T]$ are the relative displacements tangential to the interface.

The static behaviour of the discrete model at hand is now described by:

1. The constitutive equations [28,29]

$$\mathbf{e} = \mathbf{F}_0 \mathbf{s} \tag{3}$$

$$\mathbf{e} = \mathbf{e}_0 + \mathbf{e}_E + \mathbf{e}_P \tag{4}$$

$$\mathbf{e}_P = \mathbf{N}\lambda \tag{5}$$

$$\boldsymbol{\phi} = \mathbf{N}^T \mathbf{s} - \mathbf{H}\lambda - \mathbf{k} \tag{6}$$

$$\lambda \geq 0, \quad \phi \leq 0, \quad \phi^T \lambda = 0 \tag{7}$$

where $\mathbf{F}_0$ is the natural flexibility matrix of the
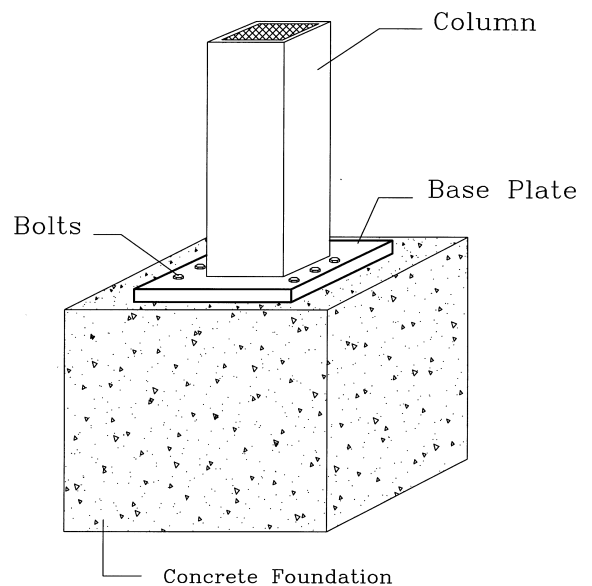
Fig. 1. The column base–plate connection.

structure, $\mathbf{e}$ the strain vector consisting of three parts, the initial strain $\mathbf{e}_0$, the elastic strain $\mathbf{e}_E$ and the plastic strain $\mathbf{e}_P$, λ is the plastic multiplier vector, ϕ the yield functions, $\mathbf{H}$ the work-hardening matrix, $\mathbf{N}$ is the matrix of the gradients of the yield functions with respect to the stresses and $\mathbf{k}$ is a vector of positive constants.

2. The equilibrium equations

$$\mathbf{Gs} = \mathbf{P} \tag{8}$$

where $\mathbf{G}$ is the equilibrium matrix and $\mathbf{P}$ the load vector.

3. The compatibility relation

$$\mathbf{e} = \mathbf{G}^T\mathbf{u} \tag{9}$$

where $\mathbf{u}$ is the displacement vector.

4. The unilateral contact conditions and the friction boundary conditions holding on the unilateral contact interfaces, as described by Eqs. (1) and (2).

A direct solution of the above problem is not possible due to the following reasons:

○ It is not a priori known which parts of the connection come into contact under the application of the static loading and which are the exact values of the contact forces.

○ For those parts that come into contact, it is not known which of them are in sticking contact or in slipping contact, i.e. for which of them the first or the second part of Eq. (2) holds, respectively.

○ Moreover, there exists an interaction between the contact and the frictional forces, i.e. the frictional forces depend on the value of the contact force, and the values of the frictional forces may alter the active contact area or the values of the contact forces.

For the above reasons the problem at hand is split into two subproblems. This procedure was first introduced in [18] for the solution of the unilateral contact problem with friction and it was mathematically investigated concerning convergence by means of a fixed point theorem [24]. The first subproblem corresponds to the problem formulated with respect to the unknowns at the direction normal to the interface, whereas the second one corresponds to the problem formulated with respect to the unknowns at the direction tangential to the interface. Consequently, the solution of the problem is achieved by applying the following iterative scheme:

1. *Contact subproblem*: first the unilateral contact problem is treated by considering that the friction forces are constant. The solution of this problem can be obtained by minimizing the potential energy of the discretized structure with the subsidiary constraint of the non-penetration condition holding on the contact interface (Eq. (1)):

$$\Pi(\mathbf{u}) = \min$$

$$\{\tfrac{1}{2}\mathbf{u}^T\mathbf{Ku} + \tfrac{1}{2}\lambda^T\mathbf{H}\lambda - \mathbf{u}^T\mathbf{GK}_0\mathbf{N}\lambda + \tfrac{1}{2}\lambda^T\mathbf{N}^T\mathbf{K}_0\mathbf{N}\lambda$$
$$+ \mathbf{e}_0^T\mathbf{K}_0(\mathbf{N}\lambda - \mathbf{G}^T\mathbf{u}) - \mathbf{P}_1^T\mathbf{u} \tag{10}$$
$$+ \mathbf{k}\lambda | \lambda \geq 0, \mathbf{u}_k \geq \mathbf{0}\}$$

where $\mathbf{P}_1$ includes both the external loading and the friction forces, assumed known, $\mathbf{K}$ is the stiffness matrix of the discrete model and $\mathbf{K}_0$ is the inverse of $\mathbf{F}_0$. The solution of the above minimization problem gives the contact and non-contact areas, the values of the contact forces S_N and the respective stress and strain states of the connection.

2. *Friction subproblem*: assuming now that the contact forces are constant and equal to the ones obtained in the previous step, the Coulomb's friction boundary conditions have also to be satisfied. The analysis problem is now formulated as a quadratic programming problem with respect to the stresses, having Eq. (2) as subsidiary conditions, i.e.

$$\Pi^C(\mathbf{s}) = \min \{\tfrac{1}{2}\mathbf{s}^T\mathbf{F}_0\mathbf{s} + \tfrac{1}{2}\lambda^T\mathbf{H}\lambda + \mathbf{s}^T\mathbf{e}|$$

$$\mathbf{N}^T\mathbf{s} - \mathbf{H}\lambda \leq \mathbf{k}, \quad \mathbf{Gs} = \mathbf{P}_2, \quad |\mathbf{S}_T| \leq \mu|\mathbf{S}_N|\} \tag{11}$$

where $\mathbf{P}_2$ includes both the external loading and the contact forces assumed as known. Problem (11) expresses the complementary energy for the problem considered, taking into account the frictional conditions on the contact interface. It is worth noting that, for the friction conditions, the formulation of the problem at hand can be done with respect to stresses and not with respect to displacements because otherwise nondifferentiable terms (due to the absolute values) appear.

The two previously described steps constitute the first iteration of the method which is repeated later. In the second double step, the unilateral static problem is solved by taking into account as *nonactive contact* and *sliding regions* those obtained in the first double step by also assuming as known the tangential loading, calculated from the previous step. In this sense, a new external loading is applied to the connection, which in turn is solved again, i.e. by first minimizing the potential energy of the structure and then minimizing its complementary energy. Obviously, the equilibrium configuration of the connection may be different between two successive solution steps. This means,
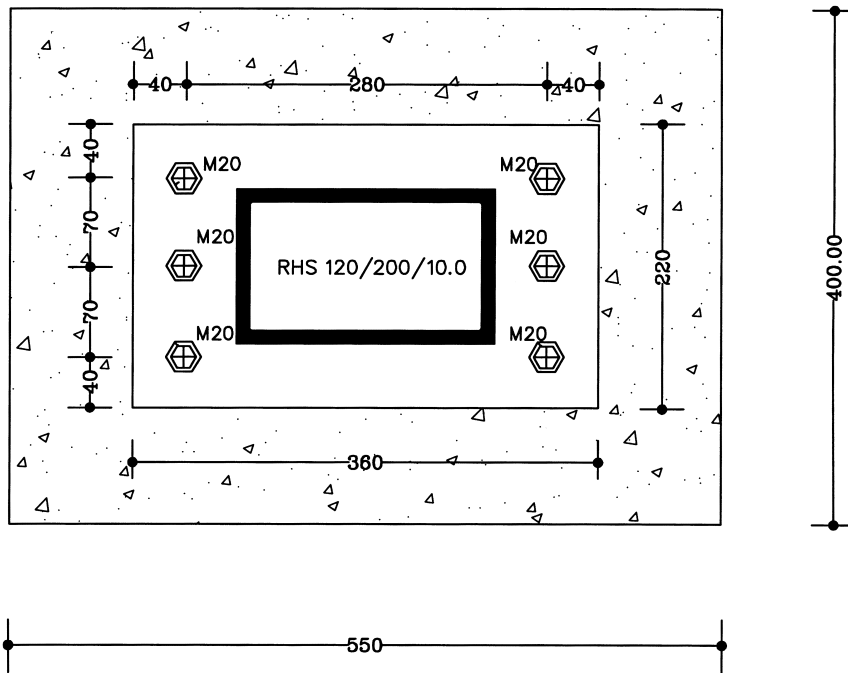
Fig. 2. Geometrical data of the considered plate connection.

that the *activated contact* and the *sliding regions* computed in the second step are probably different from those calculated in the first step. The iterative solution procedure continues by solving quadratic programming problems which keep the same basic mathematical characteristics, but take as input data the output of the previous step. This iterative procedure continues until the difference of two successive stress states of the connection is less than a desirable accuracy $\|\mathbf{s}^{(n+1)} - \mathbf{s}^{(n)}\| < \epsilon$.

Concerning the numerical treatment of the formulated quadratic programming problems, effective algorithms from the theory of optimization can be applied [30]. As for the first step of the solution procedure (i.e. computation of the active contact and separation regions between the various interfaces (Eq. (10)), the optimization algorithm explicitly determines the nodes coming into contact with the respective contact forces. Then, the optimization algorithm is applied in a similar way within the second step of the method. The post-processing part of the algorithm concerning the computation of the new stress distribution is done as in the usual finite element analysis. It is therefore obvious that the only real difference of the necessary software from classical finite element codes will be the substitution of the programming routine to solve quadratic equations and the treatment of the additional data concerning the inequality constraints.

3. Numerical applications

The developed algorithm described above is applied in order to simulate the behaviour of the base plate connection shown in Fig. 2. The connection consists of an RHS 120/200/10 steel column which is connected to a concrete block through a steel plate. The thickness of the base plate is considered as a critical parameter which varies, taking the following values: 20, 25 and 30 mm. Six M20-5.6 bolts are also used. The connection is idealized through a two-dimensional finite element mesh (Fig. 3), consisting of 4044 nodes and 2829 plane stress quadrilateral elements. The presented finite element mesh (FEM) is the final one of a series of FE meshes with different densities that were studied by the authors. Attempts to further refine the mesh gave results very close to the ones presented here.

Table 1
Equivalent thickness for the various parts of the connection

Connection element	Equivalent thickness (mm)
Concrete block	400.0
Base plate	220.0
Steel profile (weak area)	20.0
Steel profile (strong area)	120.0
Bolt	47.1
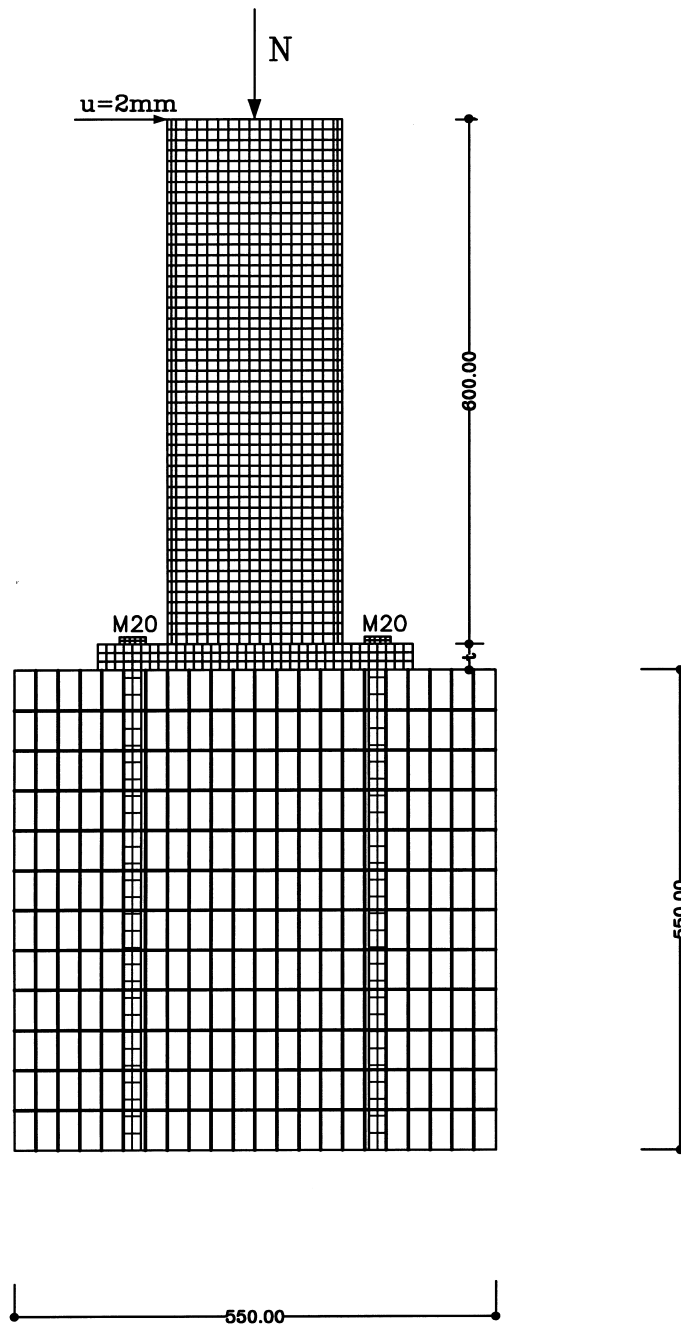
Fig. 3. Finite element mesh of the 2-D model.

Therefore, the results are considered satisfactory for the analysis and on the other hand the computational loading is reasonable. The thickness of the plane stress elements are properly adjusted in order to take into account the three-dimensional properties of the structure (Table 1). In the region of the holes of the plate, the plate and the bolt overlap. The interaction between the two bodies is taken into account by considering unilateral contact conditions between them. Unilateral contact conditions are also assumed to hold between the plate and the concrete block. The elastoplastic stress–strain law of the steel profile and the plate are given in Fig. 4. A similar diagram is used to describe the material of the bolt (Fig. 5). Finally, the material
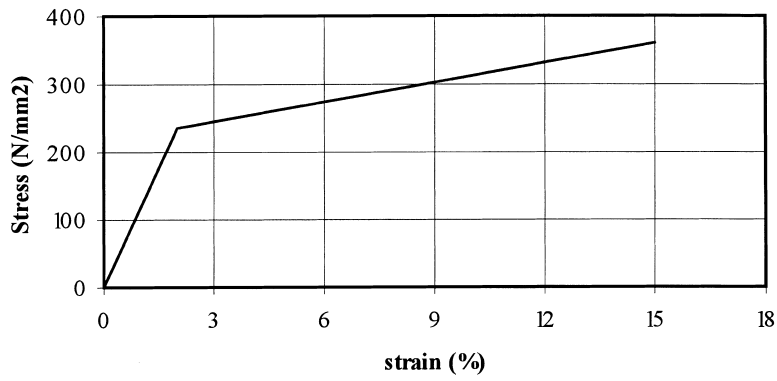
Fig. 4. Adopted stress–strain relations for the steel column and base plate connection.
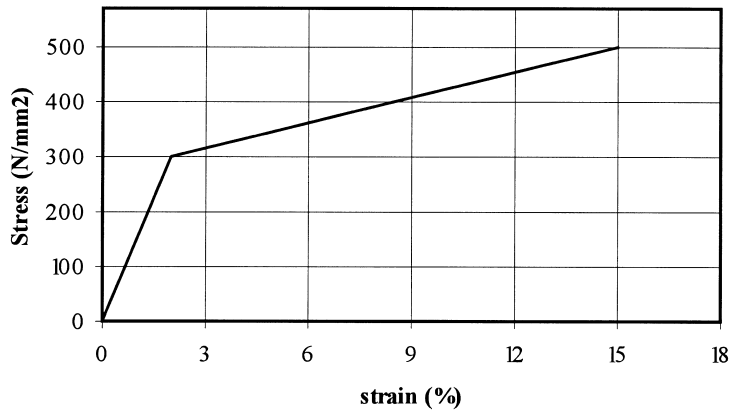
Fig. 5. Adopted stress–strain relations for the bolts.
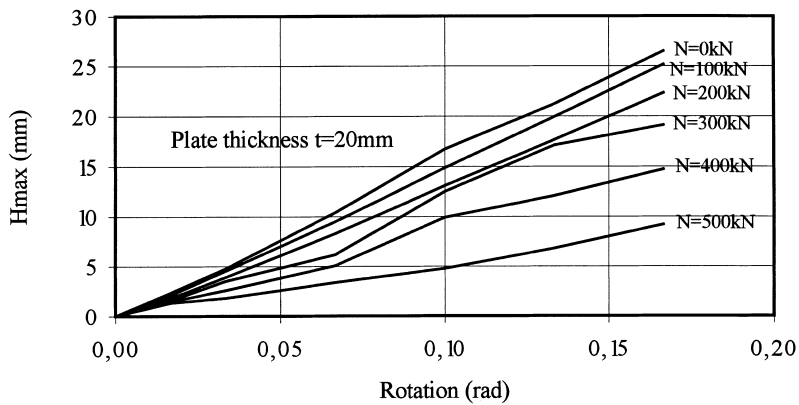
Fig. 6. Maximum node detachment—rotation diagrams for base plate thickness $t = 20$ mm.
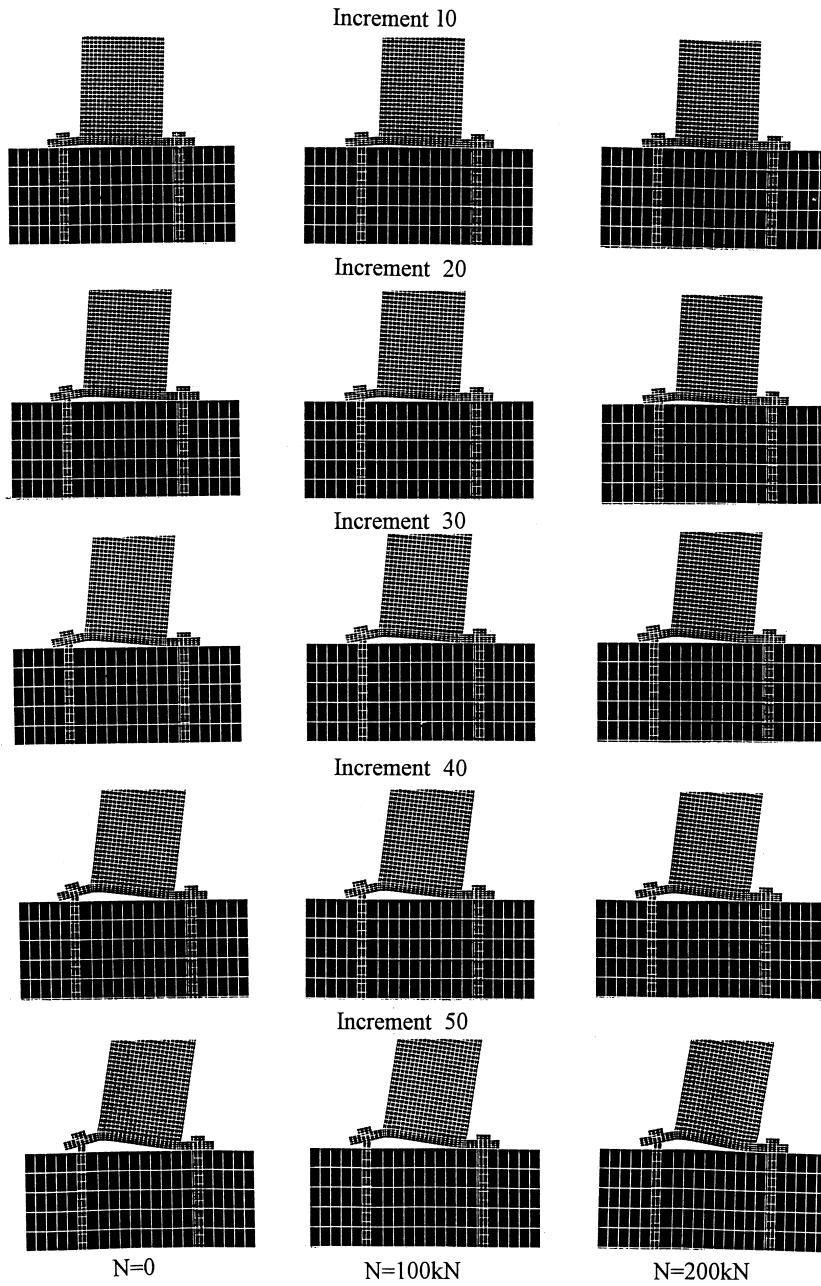
Increment 10

Increment 20

Increment 30

Increment 40

Increment 50

N=0   N=100kN   N=200kN

Fig. 7. Deformed shapes of the 20 mm base plate connection, for axial loading 0, 100 and 200 kN.

Increment 10

Increment 20

Increment 30

Increment 40

Increment 50

N=300kN   N=400kN   N=500kN
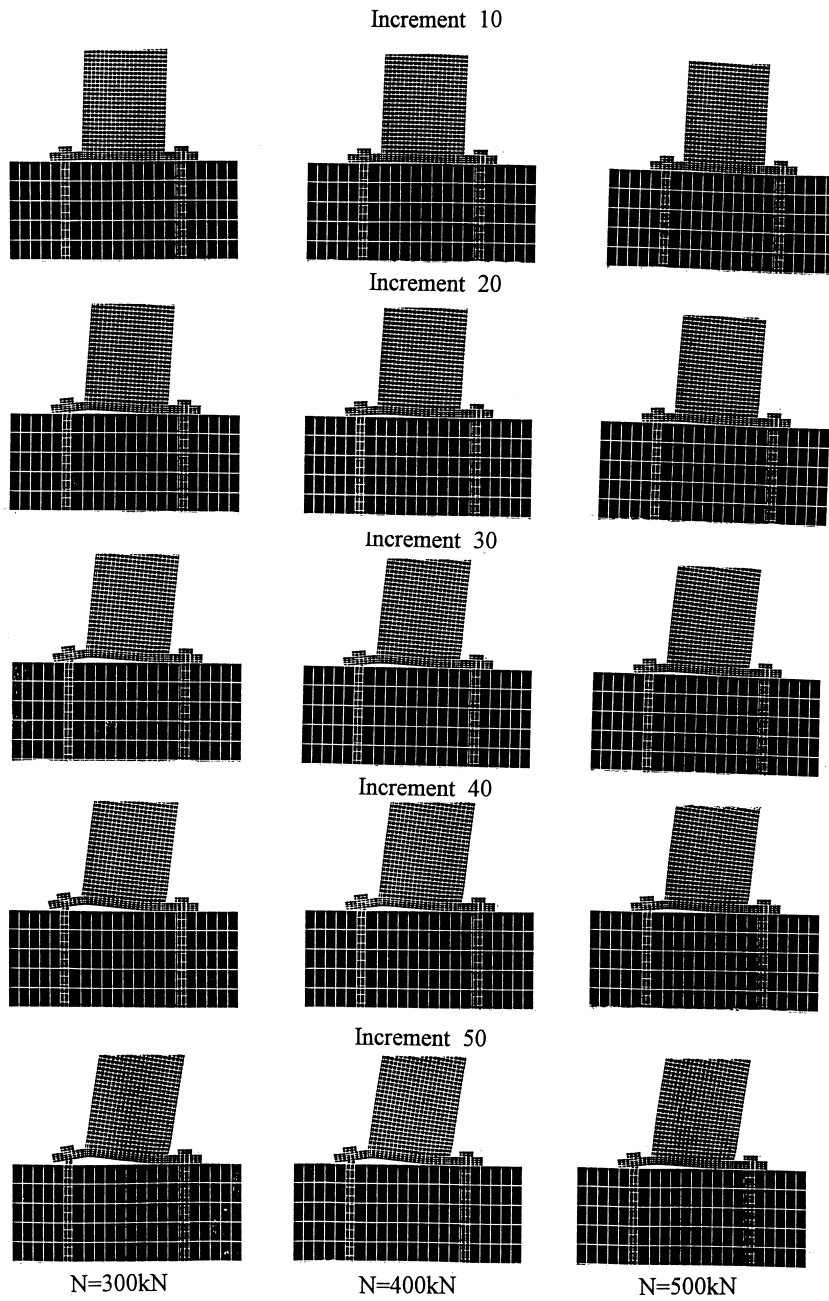
Fig. 8. Deformed shapes of the 20 mm base plate connection, for axial loading 300, 400 and 500 kN.
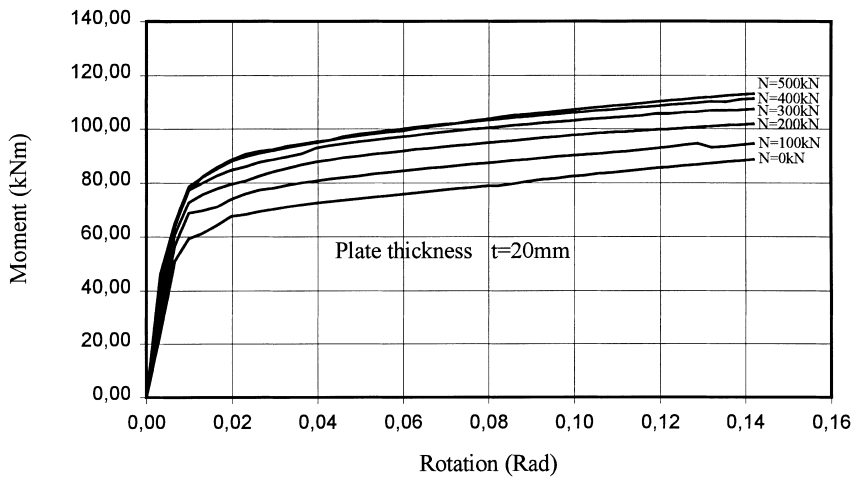
Fig. 9. Moment–rotation diagrams for the six cases of axial loading, plate thickness $t = 20$ mm.

of the concrete block is considered as linear with elasticity modulus $E_c = 29$ GPa. The friction coefficient between the base plate and the concrete is taken as equal to $\mu = 0.3$. The structure is loaded by applied displacements introduced as a sequence of 50 increments on the top of the edge of the column. At each increment a displacement of 2 mm is applied into the structure. We distinguish three sets of solutions, each one corresponding to the three above-mentioned selected plate thicknesses. In each set, the axial compressive loading of the connection consists of the following six cases: 0, 100, 200, 300, 400 and 500 kN.

4. Results for the base plate connections

From the first set of results for base plate thickness $t = 20$ mm, we notice that a contact zone is established

under the right end of the base plate. The resting part of the plate starts to separate from the concrete foundation, tensioning the left bolt. The maximum detachment of a selected base plate node near the left bolt is obtained for each increment and shown in Fig. 6, for the six cases of axial load. The deformation of the base plate as well as the plastic strains decrease as axial load increases. The opposite situation occurs for the columns, which develops greater plastic strains with the increase in the axial force. This fact is verified from the plastic strains of the base plate for the cases of axial force, 0, 100 and 200 kN, where the plastic strains in the base plate are significantly larger than in the column. In these cases the structure collapses due to the plastification of the base plate as well as the failure of the left bolt. The left bolt develops tension forces near 400 N/mm^2 at the 50th increment due to the fact that as the plate rises it causes tension at the
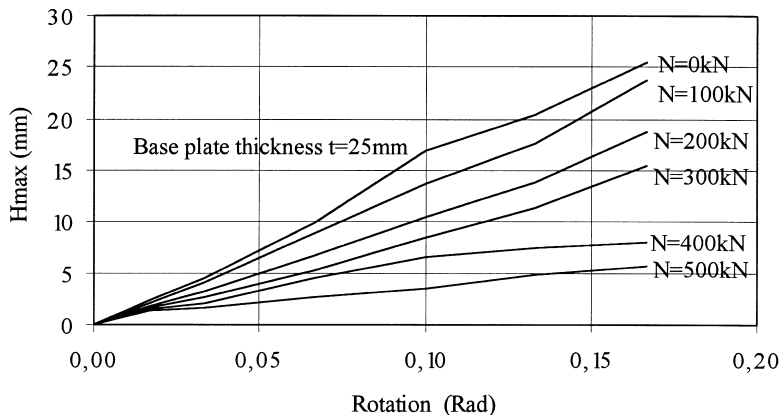
Fig. 10. Maximum node detachment—rotation diagrams for base plate thickness $t = 25$ mm.

Increment 10

Increment 20

Increment 30

Increment 40

Increment 50

N=0   N=100kN   N=200kN
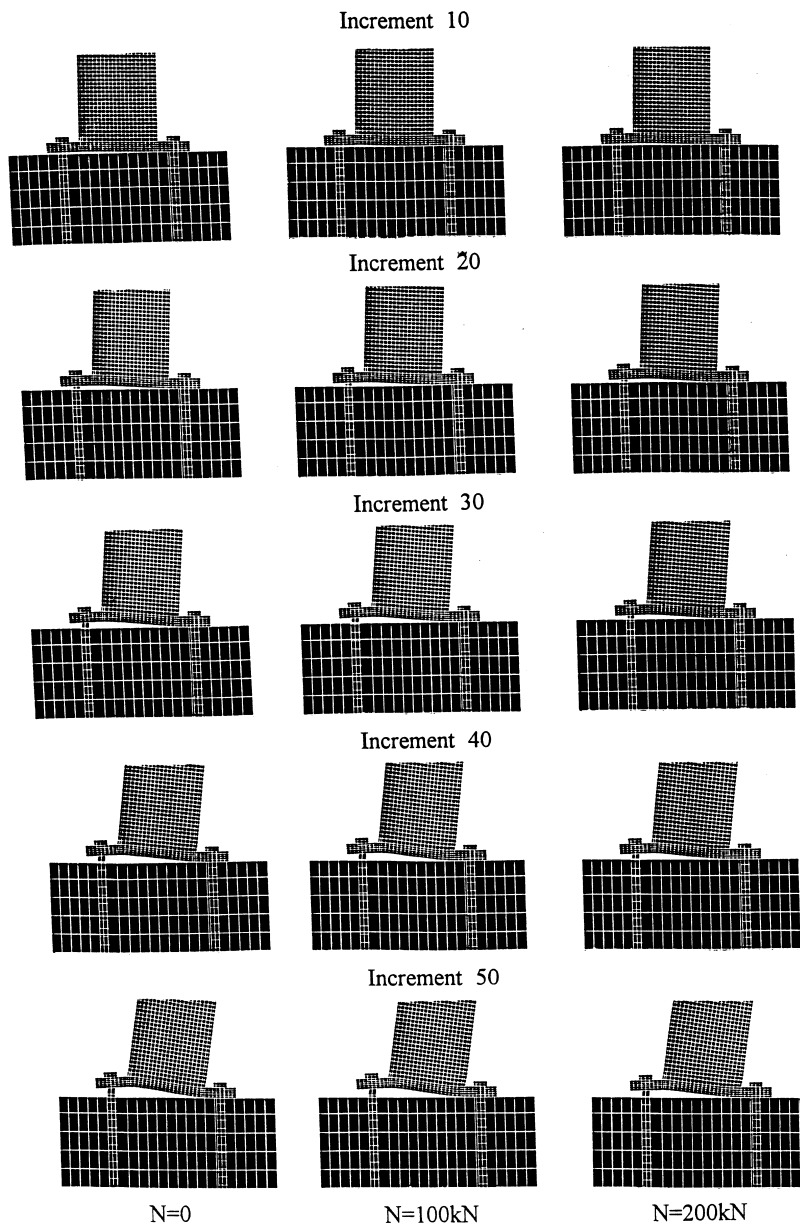
Fig. 11. Deformed shapes of the 25 mm base plate connection, for axial loading 0, 100 and 200 kN.

left bolt, creating an additional critical member failure. For the applied axial force 300 kN, the plastic strains are similar in the column and base plate and finally for the load cases of 400 and 500 kN the plastic strains of the column are larger, leading the RHS column to fail first, developing plastic hinges at the lower parts of the edges of the steel column. Figs. 7 and 8 give the deformed shapes of the connection for the six cases of axial loading at increments 10, 20, 30, 40 and 50. From the deformed shapes it is observed that the lar-

ger part of the base plate for the first 20 increments is always in contact with the concrete. For the following increments, as the base plate uplifts, only the left edge node and the base plate nodes near the right bolt remain in contact with the concrete foundation. This contact area increases along with the axial loading from 0 to 500 kN.

Concerning the stress condition of the connection, although the right region of the column and the base plate are naturally the first expected failure areas, simi-

Increment 10

Increment 20

Increment 30

Increment 40

Increment 50

N=300kN   N=400kN   N=500kN
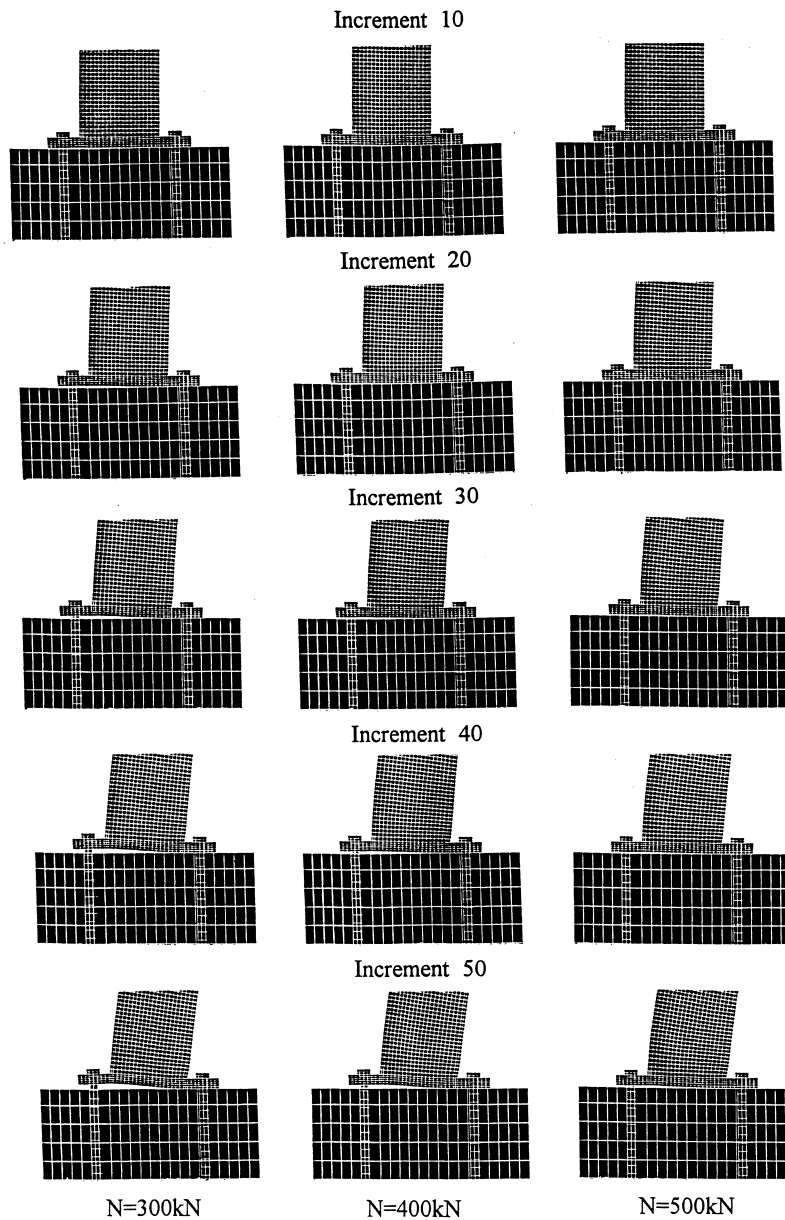
Fig. 12. Deformed shapes of the 25 mm base plate connection, for axial loading 300, 400 and 500 kN.

lar stresses are developed in the left region after the 14th–18th increments. This phenomenon occurs because of prying forces which are developed in this area, when the left edge of the base plate comes into contact with the concrete base. From the moment–rotation curves (Fig. 9) it becomes obvious that the moment capacity of the connection increases along with the increase in the axial force. For axial force 0 kN the moment capacity is near 90 kNm. In the case of 500 kN the moment capacity reaches 116 kNm.

The stress condition as well as the plastic strains for the second set of results, with base plate thickness $t = 25$ mm change because prying forces are not present in this case. Comparing this result with the model with base plate thickness $t = 20$ mm, the highest uplift is slightly smaller, as well as the separation length. These results are natural, since the stiffness of the base plate increases for thickness $t = 25$ mm, permitting smaller deformability and reducing its final plastic strain. This fact is also observed from the maximum
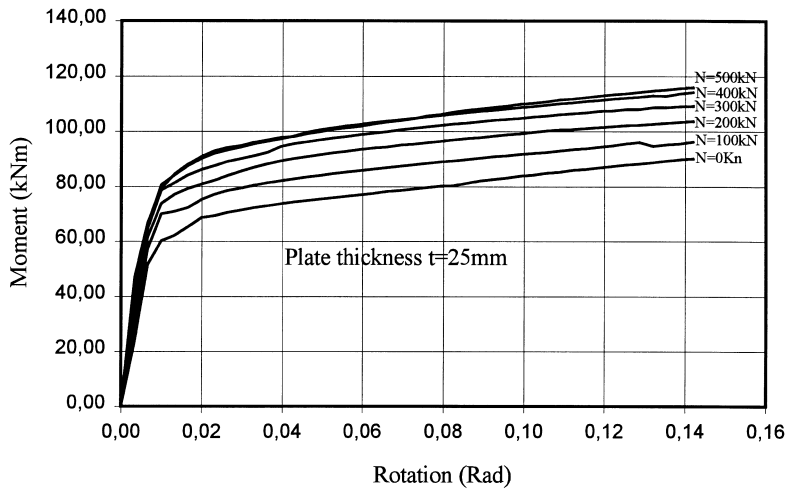
Fig. 13. Moment–rotation diagrams for the six cases of axial loading, plate thickness $t = 25$ mm.

node detachment of the base plate (Fig. 10), at the left edge of the base plate. The steel column for each case of axial force fails around the area of its right foot near the 40th increment, with stresses that exceed its ultimate strength. The stresses appearing in the left region of the base plate are beneath its ultimate strength. This occurs because the prying forces which were developed in the previous analysis for plate thickness $t = 20$ mm do not appear. Through the deformed shapes of the base plate for the six cases of axial loading at increments 10, 20, 30, 40 and 50 (Figs. 11 and 12), we notice that the bending of the base plate is reduced in comparison with the connection of plate thickness $t = 20$ mm. This proves that the increase of the stiffness of the base plate significantly affects its re-

sponse under the applied axial loading and bending moment combination.

For axial forces 0 and 100 kN the base plate and the left bolt exceed their yield strength and reach their ultimate plastic strains in a similar way to the case for the $t = 20$ mm base plate. For the remaining loads from 200 to 500 kN the column begins to plastify, creating plastified areas which, in comparison with the plate with thickness 20 mm, are slightly smaller. The other parts of the connection are not critical and still preserve strength capacity. From the moment–rotation curves (Fig. 13), for axial force 0 kN the moment capacity is near 100 kNm and in the case of 500 kN the moment capacity reaches 120 kNm.

From the third set of results for base plate thickness $t = 30$ mm, the stress condition of the plate is similar
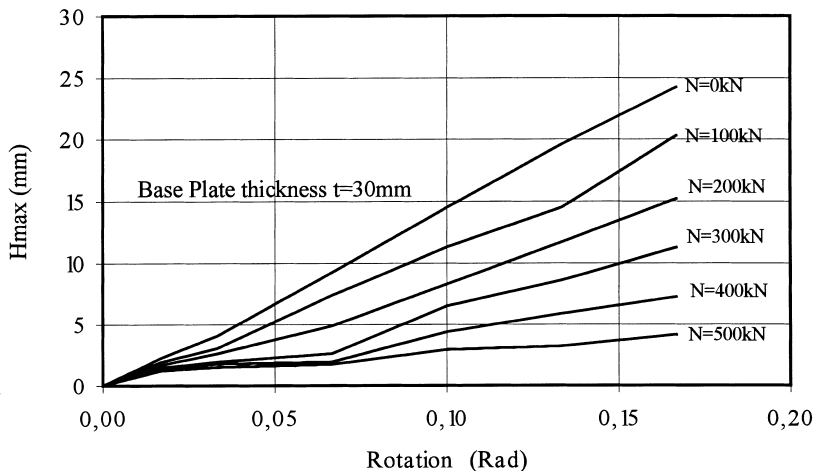
Fig. 14. Maximum node detachment—rotation diagrams for base plate thickness $t = 30$ mm.

Increment 10

Increment 20

Increment 30

Increment 40

Increment 50

N=0   N=100kN   N=200kN
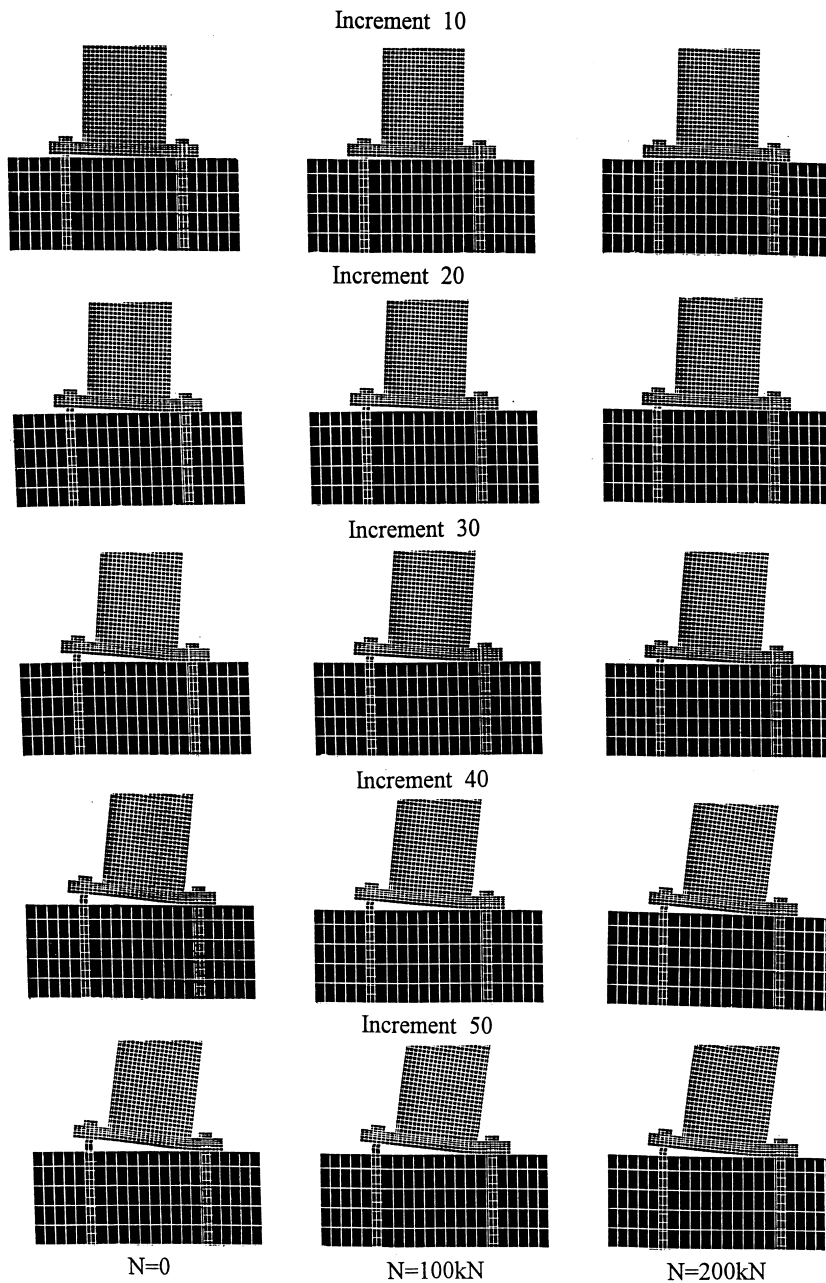
Fig. 15. Deformed shapes of the 30 mm base plate connection, for axial loading 0, 100 and 200 kN.

to the case of plate thickness $t = 25$ mm, because the prying forces are not present. Increasing the base plate thickness, the stiffness it possesses permits limited deformation which is slightly visible only for the last increments. As a result, the base plate does not fail for any case of axial load. Significant stresses are developed mainly at the area of the right foot of the column, which fails first, exceeding its ultimate plastic strain. Fig. 14 provides us with a full picture of the maximum detachment of the node at the left edge of the base plate. In comparison with the previous plate thickness, 20 and 25 mm, the maximum height the plate rises is smaller, especially in the case of axial force 500 kN. Figs. 15 and 16 present the deformation of the connection for six cases of axial loading at increments 10, 20, 30, 40 and 50. For all the cases of

Increment 10

Increment 20

Increment 30

Increment 40

Increment 50

N=300kN   N=400kN   N=500kN
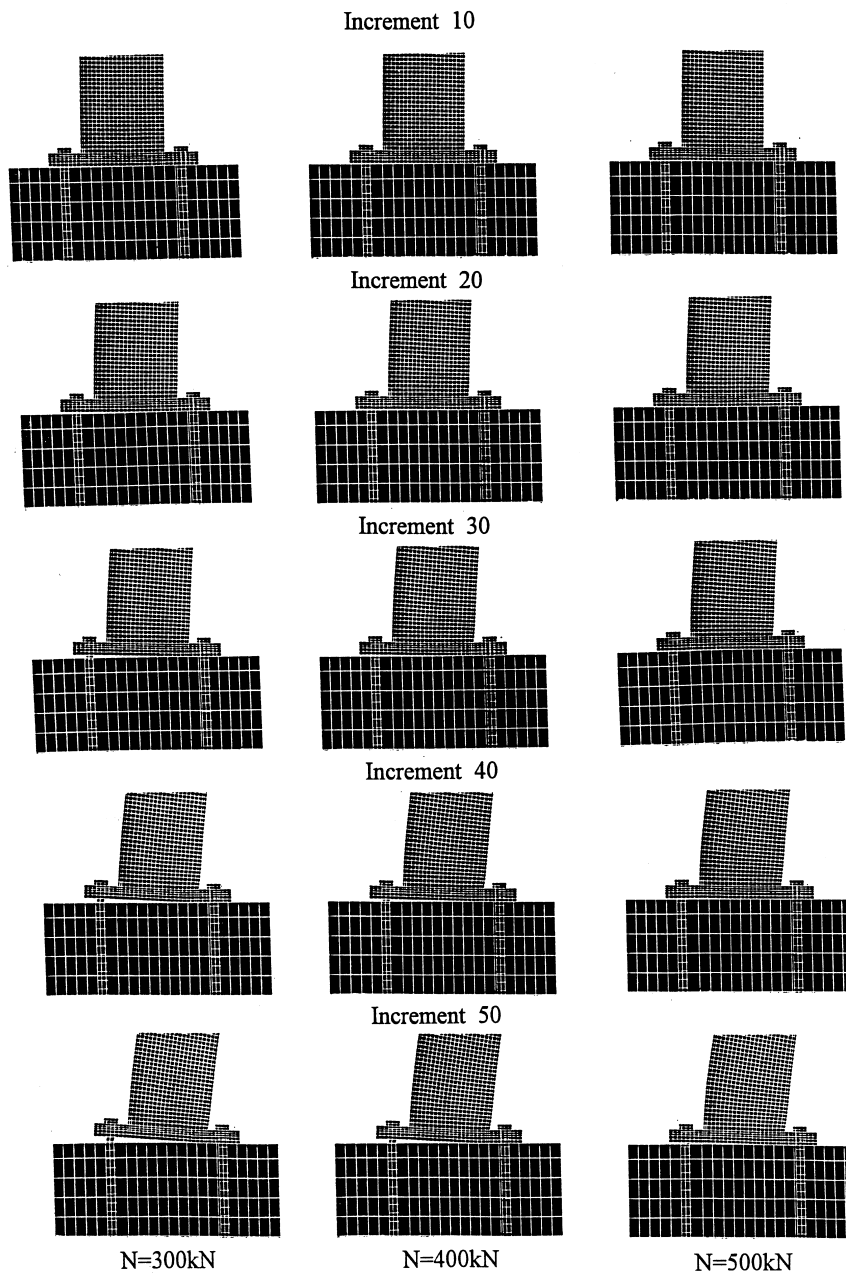
Fig. 16. Deformed shapes of the 30 mm base plate connection, for axial loading 300, 400 and 500 kN.

loading, the column fails after the 40th increment. The developed plastic areas create a plastic hinge at the lower right part of the steel column. Thus the collapse of the structure occurs due to the plastification of the steel column and the other parts of the connection are not critical. The obtained moment–rotation curves (Fig. 17) are similar to the previous cases. For axial force 0 kN, the moment capacity is near 100 kNm. In

the case of 500 kN, the moment capacity reaches 125 kNm.

5. Concluding remarks

This study investigates the structural response of column–base plate connections by means of a two-
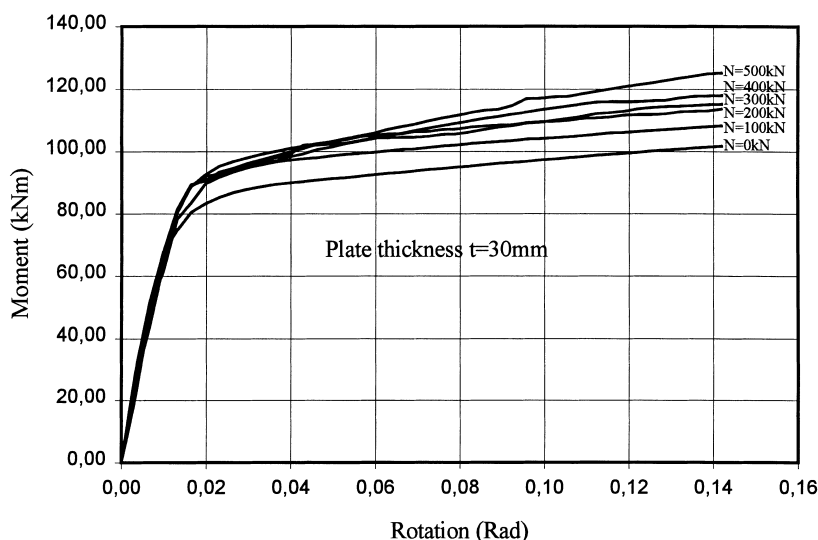
Fig. 17. Moment–rotation diagrams for the six cases of axial loading, plate thickness $t = 30$ mm.

dimensional model within a nonsmooth mechanics theoretical framework. The parametric analysis of the model shows that the stiffness of the base plate is a significant parameter, affecting the development of prying action at the active contact areas of the plate. The appearance of prying forces creates plastification zones at the interfaces of the connections, in areas that could not be considered using classical design and calculation methods. The reader should have in mind that a two-dimensional model is analysed instead of a more accurate three-dimensional model (obviously more subtle processes, e.g. a cone mechanism cannot be predicted). We should notice here that a two-dimensional analysis encompasses all the essential characteristics and dominant plastification mechanisms of the problem considered with the given geometry. Indeed, the equivalent T-stub model (which is also used for the structural verification of the base plate connection according to Eurocode 3) collapses in mode I (complete flange yielding), which means that two plastic hinges are developed. As a consequence, the whole structure is in a more or less two-dimensional deformed configuration, something that justifies the validity of the assumptions that led to the present model.

Acknowledgements

References

[1] Fling RS. Design of steel bearing plates. Engng J AISC 1970;7:37–40.

[2] Stockwell Jr FW. Preliminary base plate selection. Engng J AISC 1975;12:92–9.

[3] Murray TM. Design of lightly loaded steel column base plates. Engng J. AISC 1983;20:92–99 143–152.

[4] Dewolfe JT. Axially loaded column base plates. J Struct Div ASCE 1978;104:781–94.

[5] Dewolfe JT, Sansley EF. Column base plates with axial loads and moments. J Struct Div ASCE 1983;106:2167–84.

[6] Thambiratnam DP, Paramasivam P. Base plates under axial loads and moments. J Struct Div ASCE 1986;112:1166–81.

[7] Cook RA, Klinger RE. Ductile multiple-anchor steel-to-concrete connections, J. Struct. Div. ASCE 118:1645–1665.

[8] Krishnnamurthy N. A fresh look at bolted steel end-plate behavior and design. Engng J AISC 1978;15:39–49.

[9] Krishnnamurthy N, Graddy DD. Correlation between 2- and 3-dimensional finite element analysis of steel bolted end-plate connections. Compu Struct 1976;6:381–9.

[10] Kato B, McGuire W. Analysis of T stub flange to column connection. J Struct Div ASCE 1973;99:865–88.

[11] Paker SA, Morris LJ. A limit state design method for tension of bolted column connections. Struct Engnr 1977;55:876–89.

[12] Kukreti AR, Murray TM, Abolmaali A. Endplate connection moment-rotation relationship. J Construct Steel Res 1987;8:137–57.

[13] Chen WF, Patel KV. Static behaviour of beam-to-column moment. J Struct Div ASCE 1981;197:1815–38.

[14] Chen WF, Lui EM. Steel beam-to-column moment connections. Part I: flange moment connections. S M Arch 1986;11:257–316.

[15] Bortman J, Szabó BA. Nonlinear models for fastened structural connections. Comput Struct 1992;43:909–1023.

[16] Thambiratnam DP, Krishnnamurthy N. Computer analysis of column base plates. Comput Struct 1989;33:839–50.

[17] Baniotopoulos CC, Karoumbas G, Panagiotopoulos PD. A contribution to the analysis of steel connections by means of quadratic programming techniques. In: Proceedings of 1st European Conference on Numerical Methods in Engineering. Amsterdam: Elsevier, 1992. p. 519–525.

[18] Panagiotopoulos PD. A nonlinear programming approach to the unilateral contact and friction boundary value problem in the theory of elasticity. Ing Archiv 1975;44:421–32.

[19] Panagiotopoulos PD. Inequality problems in mechanics and applications: Convex and nonconvex energy functions. Basel: Birkhäuser, 1985.

[20] Thomopoulos K. Improvement of the design method for steel column baseplates via an inequality approach. Civil Engrg Pract Des Engns 1985;4:923–33.

[21] Baniotopoulos CC. On the numerical assessment of the separation zones in semirigid column base plate connections. Struct Engng Mech 1994;2:1–15.

[22] Baniotopoulos CC. On the separation process in bolted steel splice plates. J Construct Steel Res 1995;32:15–35.

[23] Baniotopoulos CC, Abdalla KM. Steel column-to-column connections under combined load: a quadratic programming approach. Comput Struct 1993;46:13–20.

[24] Nečas J, Jarusek J, Haslinger J. On the solution of the variational inequality to the signorini problem with small friction. Bull UMI 1980;17B:796–811.

[25] Mistakidis ES, Baniotopoulos CC, Bisbos CD, Panagiotopoulos PD. A 2-D numerical method for the analysis of steel T-stub connections. In: Proceedings of 2nd National (Greek) Conference on Computational Mechanics, Chania, 1996. p. 777–84.

[26] Jaspart JP. 1994 Numerical simulation of a T-stub—Experimental Data. COST C1—numerical simulation working group. C1WD6/94/091–9.

[27] Mistakidis ES, Baniotopoulos CC, Panagiotopoulos PD. A numerical method for the analysis of semirigid base-plate connections. In: Proceedings ECCOMAS 96. New York: Wiley, 1996. p. 842–8.

[28] Maier G. A quadratic programming approach for certain classes of nonlinear structural problems. Meccanica 1968;2:121–30.

[29] Panagiotopoulos PD, Baniotopoulos CC, Avdelas A. Certain propositions on the activation of yield modes in elastoplasticity and their applications to deterministic and stochastic problems. ZAMM 1984;64:491–501.

[30] Fletcher R. Practical optimization methods. New York: Wiley, 1987.